Molecular Therapy
Nucleic Acids
Original Article

Activation of AMPK Attenuated Cardiac Fibrosis by Inhibiting CDK2 via p21/p27 and miR-29 Family Pathways in Rats

Hanping Qi,[1,4] Yan Liu,[1,4] Shuzhi Li,[1] Yunping Chen,[1] Lei Li,[2] Yonggang Cao,[1] Mingyao E,[1] Pilong Shi,[1] Chao Song,[1] Baiyan Li,[3] and Hongli Sun[1]

[1]Department of Pharmacology, Harbin Medical University-Daqing, Daqing, Heilongjiang 163319, China; [2]Department of Orthopedics, Fifth Clinical College of Harbin Medical University, Daqing, Heilongjiang 163316, China; [3]Department of Pharmacology, Harbin Medical University, Harbin, Heilongjiang 150081, China

Cardiac fibrosis is pathological damage associated with nearly all forms of heart disease. AMP-activated protein kinase (AMPK) is an evolutionary conserved energy-sensing enzyme. Emerging evidences indicate that AMPK plays an important role in cardiac fibrosis and cell proliferation. However, less is known about the detailed mechanism of AMPK activation on cardiac fibrosis. In this study, we found the AMPK activation improved the impaired cardiac function of cardiac fibrosis rats and decreased interstitial fibrosis. Further results indicated AMPK activation promoted p21 and p27 and inhibited CDK2 and cyclin E protein expressions both in vivo and in vitro. Moreover, AMPK activation repressed downstream transcription factor hepatocyte nuclear factor 4 alpha (HNF-4α) expression and decreased the binding of HNF-4α to TGF-β_1 promoters, which eventually resulted in TGF-β_1 downregulation and miR-29 family upregulation. Furthermore, miR-29, in turn, inhibited the progression of cardiac fibrosis through suppressing its target CDK2. Taken together, activation of AMPK, on the one hand, upregulated p21 and p27 expression, further inhibited CDK2 and cyclin E complex, and finally suppressed the progression of cardiac fibrosis, and, on the other hand, repressed HNF-4α expression, further downregulated the activity of TGF-β_1 promoter, promoted miR-29 expression, and finally prevented the development of cardiac fibrosis.

INTRODUCTION

Cardiac fibrosis is an irreversible and progressive end-organ damage of the heart, which caused a significant global health problem associated with nearly all forms of heart disease.[1] An important event in cardiac fibrosis is the transformation of fibroblasts into myofibroblasts, which secrete large amounts of extracellular matrix proteins, and then cause cardiac fibrosis.[2] This remodeling involves pathological changes characterized by scarring, a stiffer and less compliant cardiac muscle, cardiomyocyte hypertrophy and apoptosis, and ultimately develops into heart failure. Despite the critical importance of fibrosis in cardiovascular disease, there currently are no effective cardiac fibrosis therapies available in clinical practice. Therefore, identifying molecular mechanisms mediating cardiac fibrosis and providing a new target for clinical treatment and pharmaceutical convention need to be addressed.

AMP-activated protein kinase (AMPK) is a highly conserved heterotrimeric serine/threonine kinase comprised of a single catalytic (α) subunit and two regulatory (β and γ) subunits. The classic function of AMPK is as an important fuel gauge that maintains energy homeostasis by regulation of fuel supply and energy-generating pathways.[3] It can be activated by the increase in the AMP:ATP ratio induced by hypoxia/anoxia, exercise,[4,5] muscle contraction, and metformin.[6] Recent studies have revealed an expanded role for AMPK in apoptosis,[7,8] autophagy,[9] and endoplasmic reticulum stress.[10] Aside from these roles, emerging evidence indicates that intrinsic AMPK activation also has important actions on ischemia[11] and the hypertrophic process.[12] In the mouse heart, AMPK is activated during pressure overload-induced hypertrophy. Activation of AMPK also protects cardiac ischemia/reperfusion by anti-apoptosis and inhibition of autophagy. However, the role of AMPK in protecting against cardiac fibrosis has never been elucidated.

MicroRNAs (miRNAs) are endogenous, small non-coding RNA molecules approximately 19–22 nt in length that anneal inexactly to complementary sequences in the 3′ UTRs of target mRNAs to regulate their target gene expression post-transcriptionally. Numerous studies have shown that miRNAs were involved in a wide variety of biological processes, including cell proliferation, differentiation, metastasis, apoptosis, and immune responses. It also has been reported that miRNAs participated in the regulation of pathogenesis of cardiovascular diseases, including arrhythmia,[13] cardiac hypertrophy,[14–16] and heart failure,[17] and miRNAs also were acted as prognostic markers in the development and progression of cardiovascular diseases by targeting pertinent genes. Some miRNAs were also reported to be relevant to the development and progression of cardiac fibrosis such as miR-21, miR-133, miR-30c, or miR-590. Especially, it is reported that miR-29 alleviated interstitial fibrosis in

Received 16 January 2017; accepted 5 July 2017;
http://dx.doi.org/10.1016/j.omtn.2017.07.004.

[4]These authors contributed equally to this work.

Correspondence: Hongli Sun, Department of Pharmacology, Harbin Medical University-Daqing, Daqing, Heilongjiang 163319, China.
E-mail: hlsun2002@163.com

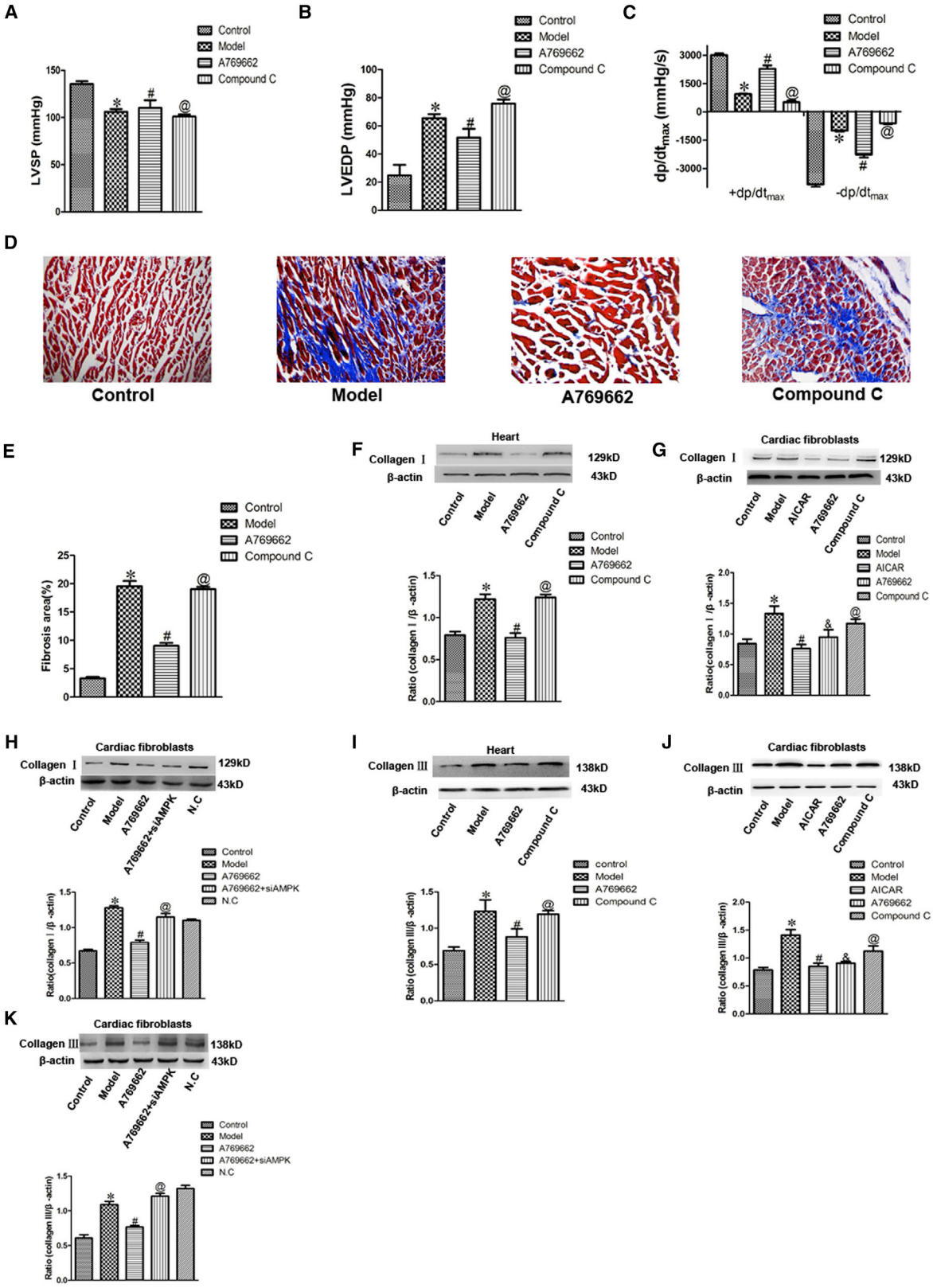

(legend on next page)

streptozotocin-induced diabetic cardiomyopathy of mice. However, how miR-29 is regulated during the pathophysiological process of cardiac fibrosis by AMPK is far from fully identified.

The aim of this study was to elucidate the essential role of AMPK in regulating cardiac fibrosis and to explore the underlying mechanism. In this study, we demonstrated that activation of AMPK has a protective effect on cardiac fibrosis by inhibition the proliferation of cardiac fibroblasts. This study suggested that activation of AMPK might be a possible therapeutic approach for cardiac fibrosis.

RESULTS

Effects of AMPK on Cardiac Function in Infarcted Rat Heart and Cardiac Interstitial Fibrosis

To investigate the effects of AMPK on cardiac function, ventricular hemodynamics were monitored after 2 weeks of A769662 (AMPK agonist) injection. As shown in Figure 1, there were significant increases in left ventricular end-diastolic pressure (LVEDP), as well as a reduction in the maximum rate of left ventricular pressure rise and fall ($\pm dp/dt_{max}$) and left ventricular systolic pressure (LVSP) in the model group ($p < 0.05$ versus control), indicating that the cardiac dysfunction was developed in all infarcted model rats. In the A769662 group, the abnormal hemodynamic parameters could be attenuated ($p < 0.05$ versus model), but these deleterious changes were further aggravated by co-treatment with compound C (AMPK antagonist) and A769662 ($p < 0.05$ versus A769662 alone). These data suggested that AMPK activation closely impacted on the cardiac function.

Interstitial fibrosis is an irresistible outcome of myocardial ischemia, leading to the increase in myocardial stiffness and decrease in cardiac compliance. Extracellular matrix (ECM) deposition in the cardiac fibrosis region was assessed using Masson's trichrome staining of the histological sections of the hearts. The results showed that the interstitial fibrotic areas of cardiac fibrosis were increased significantly compared with control rats. Interestingly, ECM deposition was obviously reduced by the treatment with A769662, and the effect of A769662 on ECM deposition could be completely reversed by compound C (Figures 1D and 1E). At the same time, to further evaluate molecular change of cardiac fibrosis, fibrous structural proteins collagen I and III were detected in vivo (heart) and in vitro (cardiac fibroblasts) in the presence of 5-aminoimidazole-4-carboxamide1-β-D-ribofuranoside (AICAR) and A769662 (AMPK activator), and the data showed that both collagen I and III expressions were dramatically upregulated in the model rats and significantly downregulated by AICAR and A769662, respectively, whereas compound C or siAMPK could reverse the action of AICAR and A769662 (Figures 1F–1K). These data suggested that the beneficial effect of AMPK activation on cardiac function might be due at least in part to the reduction of ECM deposition by downregulation of collagen expression.

Effects of AMPK Activation on Cardiac Fibroblasts Cell Cycle Progression

Cardiac fibrosis was mainly characterized by abnormal proliferation of cardiac fibroblasts. To determine whether AMPK activation inhibits the progression of cardiac fibrosis, the cardiac fibroblasts cell cycle was examined by the treatment with various concentrations of AICAR, and the results demonstrated that cardiac fibroblasts were arrested in the G_0/G_1 phase, as manifested by an increase in the percentage of cells in G_0/G_1 (Figure 2B) with a corresponding decline in the fraction of cells in S (Figure 2C) and G_2/M (Figure 2D) phases. The similar tendency in the cell number was also observed within the cell cycle (Figures 2E and 2F).

Effects of AMPK Activation on Cell Cycle Regulatory Proteins

To explore the mechanism by which AMPK hinders cell cycle progression of cardiac fibroblasts, we examined the effects of AICAR and A769662 on the expression of cell cycle regulatory proteins. Surprisingly, AICAR and A769662 dramatically decreased the expression of cyclin-dependent kinase 2 (CDK2) and cyclin E in both tissue and cell preparation compared with the model group, but these effects of AICAR and A769662 were inhibited in compound C and the A769662 + siAMPK group (Figures 3A–3F; $p < 0.05$). In addition, we further examined the CDK2 and cyclin E upstream proteins p21 and p27 to confirm the involvement of AMPK in regulating cardiac fibroblasts. We found that AICAR and A769662 significantly increased the expressions of p21 and p27 in cardiac fibrosis of rat hearts and cultured cardiac fibroblasts with Ang II, respectively. However, the effects of AICAR and A769662 were inversed by AMPK-selective antagonist compound C or silencing AMPK (Figures 3G–3l; $p < 0.05$).

To further confirm the AMPK regulation to cardiac fibroblasts via cell cycle pathway, we silenced p21 and p27 to test whether AMPK regulates these cyclin-dependent kinase inhibitors in mediating the inhibition of cardiac fibroblast proliferation. We found that small interfering RNA (siRNA) targeting p21 or p27 suppressed the AICAR-induced expression of p21 or p27, respectively, whereas the control non-targeting siRNA had no effect on the expression of either protein (Figure S1). The knock down of either p21 or p27 partially restored DNA synthesis, whereas the knock down of both p21 and

Figure 1. Effects of AMPK on Hemodynamics and Interstitial Fibrosis

(A–C) The hemodynamic parameters LVSP (A), LVEDP (B), and $+dp/dt_{max}$ and $-dp/dt_{max}$ (C) were measured throughout the experiment. LVSP: left ventricular systolic pressure; LVEDP: left ventricular end-diastolic pressure; $+dp/dt_{max}$ and $-dp/dt_{max}$: maximum rate of left ventricular pressure rise and fall. (D) Masson's trichrome staining was used to detect fibrosis (×200). The interstitial fibrosis was in blue staining. (E) Quantification of fibrosis. (F–K) The expressions of collagen I (F–H) and collagen III (I–K) proteins were measured in cardiac fibrosis rat hearts induced by left coronary artery ligation and cultured cardiac fibroblasts challenged by Ang II 100 nmol/L. siAMPK + A769662 group: cardiac fibroblasts were transfected with siAMPK for 24 hr before exposure to 300 μmol/L A769662 for 24 hr, following 24 hr treatment with Ang II and NC group: cells were transfected with a random sequence for 24 hr after treatment with Ang II for 24 hr. The data were represented by mean ± SEM. $^{*}p < 0.05$ versus control group; $^{\#}$ or $^{\&}p < 0.05$ versus model group; and $^{@}p < 0.05$ versus A769662 or AICAR group.

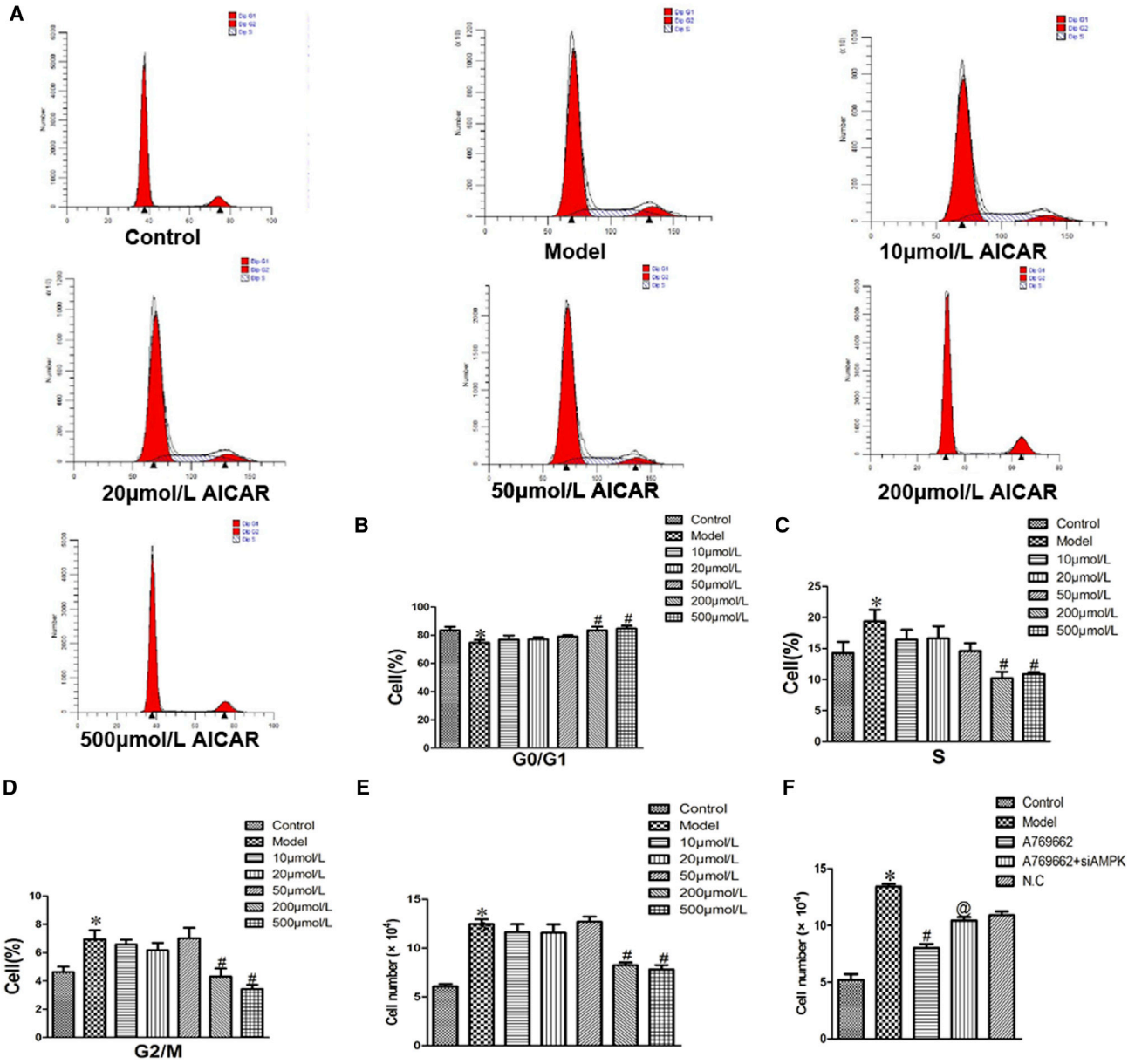

Figure 2. Activation of AMPK Inhibited Cardiac Fibroblasts Cell Cycle Progression and Number Induced by Ang II

(A) Representative histograms of cardiac fibroblasts incubated in the absence or presence of AICAR (10, 20, 50, 200, and 500 μmol/L) for 24 hr. (B–D) Effects of AICAR (10, 20, 50, 200, and 500 μmol/L) exposed for 24 hr on the distribution of cardiac fibroblasts in the G1 stage (B), S stage (C), and G2 stage (D). (E) Effects of AICAR (10, 20, 50, 200, and 500 μmol/L) exposed for 24 hr on the number of cardiac fibroblasts. (F) Effects of A769662 (another AMPK agonist) on the number of cardiac fibroblasts. siAMPK + A769662 group: cardiac fibroblasts were transfected with siAMPK for 24 hr before exposure to 300 μmol/L A769662 for 24 hr, following 24 hr treatment with Ang II and NC group: cells were transfected with a random sequence for 24 hr after treatment with Ang II for 24 hr. The results are mean ± SEM. $^{*}p < 0.05$ versus control group; $^{\#}p < 0.05$ versus model group; and $^{@}p < 0.05$ versus A769662 group.

p27 further returned the proliferative response of AICAR-treated cardiac fibroblasts (Figure 3M).

Effects of AMPK on the Expression of miR-29 Family and TGF-β_1

Here, to detect the relationship between AMPK and the miR-29 family and the transforming growth factor β_1 (TGF-β_1) signal pathway, the expression of miR-29 family and TGF-β_1 was assessed by quantitative real-time PCR and western blot, respectively. Our results revealed that activation of AMPK significantly increased miR-29a, b, and c expressions (Figures 4A–4C), as well as decreased the expression of TGF-β_1 (Figures 4D–4F). But, the action of AMPK was abolished by compound C or silencing AMPK. This result indicated that

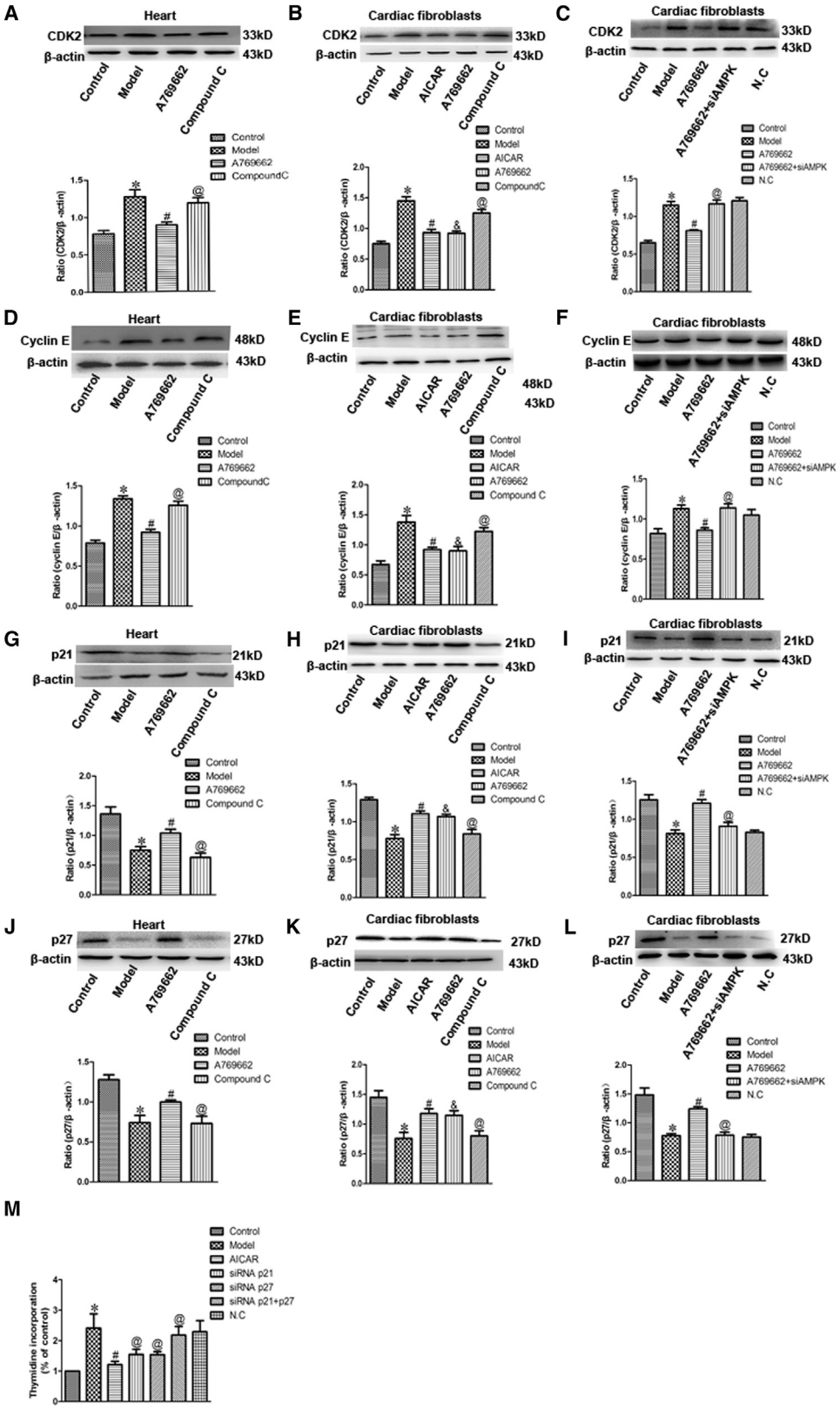

(legend on next page)

AMPK might promote miR-29a, b, and c transcription by restraining the level of TGF-β_1.

miR-29 Family Anti-fibrotic Effects through Directly Targeting CDK2

van Rooij et al.[17] reported that the miR-29 family acted as a regulator of cardiac fibrosis by the reduction of collagen expression. In our study, the effect of the miR-29 family on neonatal cardiac fibroblast proliferation was evaluated by cell counting and 3-(4, 5-dimethylthiozol-2-yl)-2, 5-diphenyltetrazo-lium bromide (MTT) assay. Treatment of cardiac fibroblasts with 100 nmol/L Ang II led to a significant increase in cardiac fibroblast proliferation, which was inhibited by overexpression of the miR-29 family (50 nmol/L), whereas co-transfection with antisense inhibitor oligonucleotide (AMO)-miR-29a, b, and c (100 nmol/L, the specific inhibitor of the miR-29 family) abrogated the effects of the miR-29 family (Figures 5A and 5B). Similarly, Ang II (100 nmol/L) elevated the protein levels of collagen I and III. Transfection with the miR-29 family (50 nmol/L) suppressed Ang II-induced collagen I and III upregulations, which were abolished by co-transfection of AMO-miR-29 (Figures 5C and 5D).

In the subsequent experiments, we further used miRanda software to predict a conserved binding site for the miR-29 family in the 3′ UTR of the CDK2 gene (Figure S2). To test this binding profile, the miR-29 family was transfected into cultured cardiac fibroblasts, and the results showed that the protein levels of CDK2 induced by Ang II were remarkably reduced. Conversely, CDK2 was significantly upregulated when AMO-miR-29a, b, and c were transfected into cardiac fibroblasts, indicating that CDK2 was negatively regulated by miR-29a, b, and c (Figure 5E). To further verify that the miR-29 family directly targets CDK2, we prepared luciferase constructs carrying the CDK2 3′ UTR (Figure 5F). Co-transfection of the miR-29 family with the luciferase reporter vector into HEK293 cells caused a sharp decrease in luciferase activity compared with transfection of the luciferase vector alone. The miR-29 family-induced depression of luciferase activity was rescued by an AMO (AMO-miR-29a, b, and c) used to delete miR-29a, b, and c. These results experimentally revealed that CDK2 was a direct target of miR-29a, b, and c.

TGF-β_1 Inhibited the Expression of miR-29 Family

Ramdas et al.[18] reported that TGF-β_1 promoted the pathological process of renal fibrosis by regulating the miR-29 family. In our present study, we found that the expression of miR-29a, b, and c were dramatically inhibited in TGF-β_1-treated cardiac fibroblasts, however, this effect could be reversed by SB525334 (TGF-β_1 receptor antagonist; Figures 6A–6C). Our result is consistent with Ramdas et al.[18]

Effects of AMPK on the Activity of HNF-4α in Neonatal Rat Cardiac Fibroblasts

To understand another signal pathway associated with the cardiac fibroblasts cell cycle regulated by AMPK, we examined the expression of the AMPK downstream transcription factor hepatocyte nuclear factor 4 alpha (HNF-4α). As shown in Figure 7, AICAR and A769662 could significantly inhibit the expression of HNF-4α in vivo and in vitro compared with the model group. The effects of AICAR and A769662 could be reversed by compound C or silencing AMPK.

HNF-4α Transcriptionally Regulated TGF-β_1 Expression by Directly Targeting the TGF-β_1 Promoters

To determine whether TGF-β_1 was transcriptionally activated by HNF-4α, we constructed luciferase reporter plasmids containing a wild-type or mutant HNF-4α-binding site at −1,756 bp-+250 bp upstream of TGF-β_1 coding sequences (Figure 8A). Luciferase reporter assays revealed that the wild-type TGF-β_1 promoters displayed significantly higher activity following HNF-4α expression in cardiac fibroblasts compared with the mutant constructs (Figure 8B). In addition, chromatin immunoprecipitation (ChIP) analyses revealed that HNF-4α could specifically bind to the TGF-β_1 promoters in cardiac fibroblasts (Figures 8C and 8D), providing strong evidence that HNF-4α could directly regulate TGF-β_1.

DISCUSSION

Ischemic cardiac fibrosis is accompanied by a variety of cellular and molecular changes that lead to inappropriate interstitial collagen formation and subsequent ventricular dysfunction.[19] Numerous approaches for inhibition of ischemic cardiac fibrosis have been described.[20–22] However, very little is known about the role of

Figure 3. Activation of AMPK Suppressed the Expressions of CDK2 and Cyclin E, as well as Promoted p21 and p27 Expressions in Cardiac Fibrosis Rat Hearts and Cultured Cardiac Fibroblasts, and Inhibited Cardiac Fibroblasts Proliferation Depended on p21 and p27 Protein Expression

The protein expressions were detected in cardiac fibrosis rat hearts induced by left coronary artery ligation and cultured cardiac fibroblasts administrated with Ang II 100 nmol/L. (A) Western blot assay for CDK2 expression in rat hearts with A769662 and compound C. (B) Western blot assay for CDK2 expression in cultured cardiac fibroblasts with AICAR, A769662, and compound C. (C) Western blot assay for CDK2 expression in cultured cardiac fibroblasts with A769662 and siAMPK. (D) Western blot assay for cyclin E expression in rat hearts with A769662 and compound C. (E) Western blot assay for cyclin E expression in cultured cardiac fibroblasts with AICAR, A769662, and compound C. (F) Western blot assay for cyclin E expression in cultured cardiac fibroblasts with A769662 and siAMPK. (G) Western blot assay for p21 expression in rat hearts with A769662 and compound C. (H) Western blot assay for p21 expression in cultured cardiac fibroblasts with AICAR, A769662, and compound C. (I) Western blot assay for p21 expression in cultured cardiac fibroblasts with A769662 and siAMPK. (J) Western blot assay for p27 expression in rat hearts with A769662 and compound C. (K) Western blot assay for p27 expression in cultured cardiac fibroblasts with AICAR, A769662, and compound C. (L) Western blot assay for p27 expression in cultured cardiac fibroblasts with A769662 and siAMPK. (M) Effects of silencing p21 and/or p27 protein expression on the inhibition of DNA synthesis by AICAR were monitored. Cells were transfected with siRNA p21 (p21 siRNA; 100 nmol/L), p27 (p27 siRNA; 100 nmol/L), and/or non-targeting siRNA (NT siRNA; 100 nmol/L) for 24 hr, and then treated with AICAR (500 μmol/L) for 24 hr, at which point cells were pulsed with [^{3}H]thymidine for DNA synthesis determination. siAMPK + A769662 group: cardiac fibroblasts were transfected with siAMPK for 24 hr before exposure to 300 μmol/L A769662 for 24 hr, following 24 hr treatment with Ang II and NC group: cells were transfected with a random sequence for 24 hr after treatment with Ang II for 24 hr. The average data were represented by mean ± SEM. *$p < 0.05$ versus control group; $^{\#}$ or $^{\&}p < 0.05$ versus model group; and $^{@}p < 0.05$ versus A769662 or AICAR group.

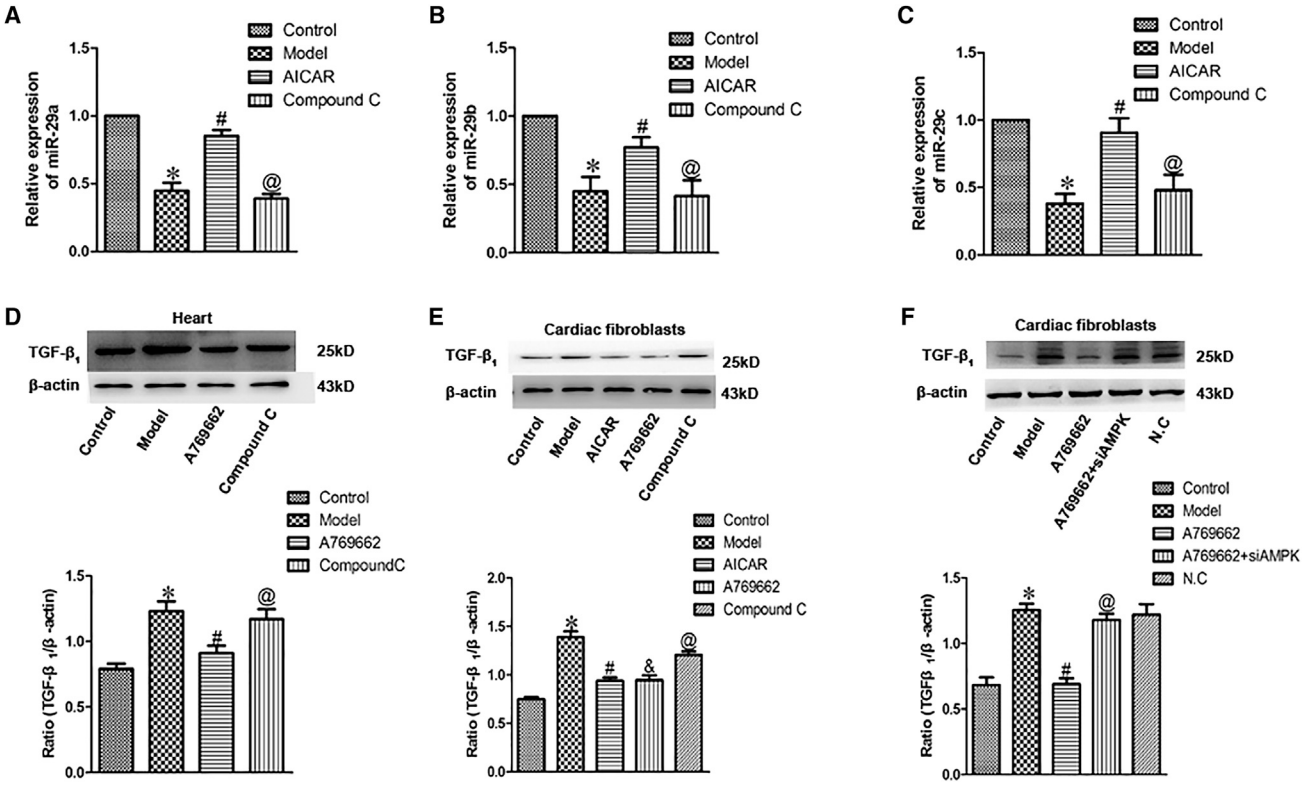

Figure 4. Activation of AMPK Promoted the Expression of miR-29 Family and Suppressed the Expression of TGF-β_1

(A–C) Activation of AMPK promoted the expressions of miR-29a (A), miR-29b (B), and miR-29c (C) in Ang II-induced cardiac fibroblasts. (D) Activation of AMPK suppressed the expression of TGF-β_1 in cardiac fibrosis rat hearts induced by left coronary artery ligation. (E) Activation of AMPK suppressed the expression of TGF-β_1 in cultured cardiac fibroblasts administrated with Ang II 100 nmol/L. (F) The inhibitory effect on TGF-β_1 expression was alleviated when silencing AMPK in cultured cardiac fibroblasts administrated with Ang II 100 nmol/L. siAMPK + A769662 group: cardiac fibroblasts were transfected with siAMPK for 24 hr before exposure to 300 μmol/L A769662 for 24 hr, following 24 hr treatment with Ang II and NC group: cells were transfected with a random sequence for 24 hr after treatment with Ang II for 24 hr. The results are mean ± SEM. *$p < 0.05$ versus control group; $^{\#}$ or $^{\&}p < 0.05$ versus model group; and $^{@}p < 0.05$ versus A769662 or AICAR group.

AMPK in cardiac fibrosis induced by left coronary artery ligation as yet. In the present study, we addressed the potential effect of AMPK on molecular events of cardiac fibroblasts and ventricular dysfunction after left coronary artery ligation.

The present study indicated that A769662 (AMPK agonist) significantly repressed the expression of collagen type-I and type-III protein and improved cardiac function in rats at 2 weeks after left coronary artery ligation. However, these changes could be reversed by compound C (AMPK antagonist). In addition, AICAR (another AMPK activator) also inhibited cultured cardiac fibroblast proliferation and DNA synthesis in a concentration-dependent fashion and largely reliant on AMPK activity. At same time, the effect of AICAR also was confirmed by the more selective AMPK activator A769662. These results suggested that AMPK possessed protective effects against cardiac fibrosis.

The eukaryotic cell cycle is an ordered set of events, and the cell duplicates its contents, and then divides into two daughter cells, including four main stages: G_1, S, G_2, and M.[23] At the present, cumulative evidences indicate that the whole process mainly is regulated by G_1 and G_2 checkpoints.[24] It is well known that cardiac fibrosis is characterized by cardiac fibroblasts excessive proliferation and collagen deposition, which is, therefore, a likely way to alleviate the degree of cardiac fibrosis. In our present study, analysis of the flow cytometry results indicated that the relevant AMPK activator AICAR dramatically repressed cardiac fibroblasts excessive proliferation, as well as revealed that a mass of cardiac fibroblasts were arrested in the G_0/G_1 stage within the cell cycle. It is widely accepted that cyclins and cyclin-dependent kinases (CDKs) are two key classes of regulatory molecules in the eukaryotic cell cycle.[25] Therefore, the cyclin E-CDK2 complex, which pivotally promoted the G_1-to-S transition, was examined. Our result showed that activation of AMPK significantly inhibited the expression of CDK2 and the cyclin E protein, and these changes could be reversed by compound C. These data demonstrated that AMPK activation inhibited cardiac fibroblasts excessive proliferation through blocking the cardiac fibroblasts cell cycle. We next sought the mechanism by which AMPK disrupted cell cycle progression in cardiac fibroblasts, and then we examined the effect of AICAR or A769662 on the expression of cell cycle

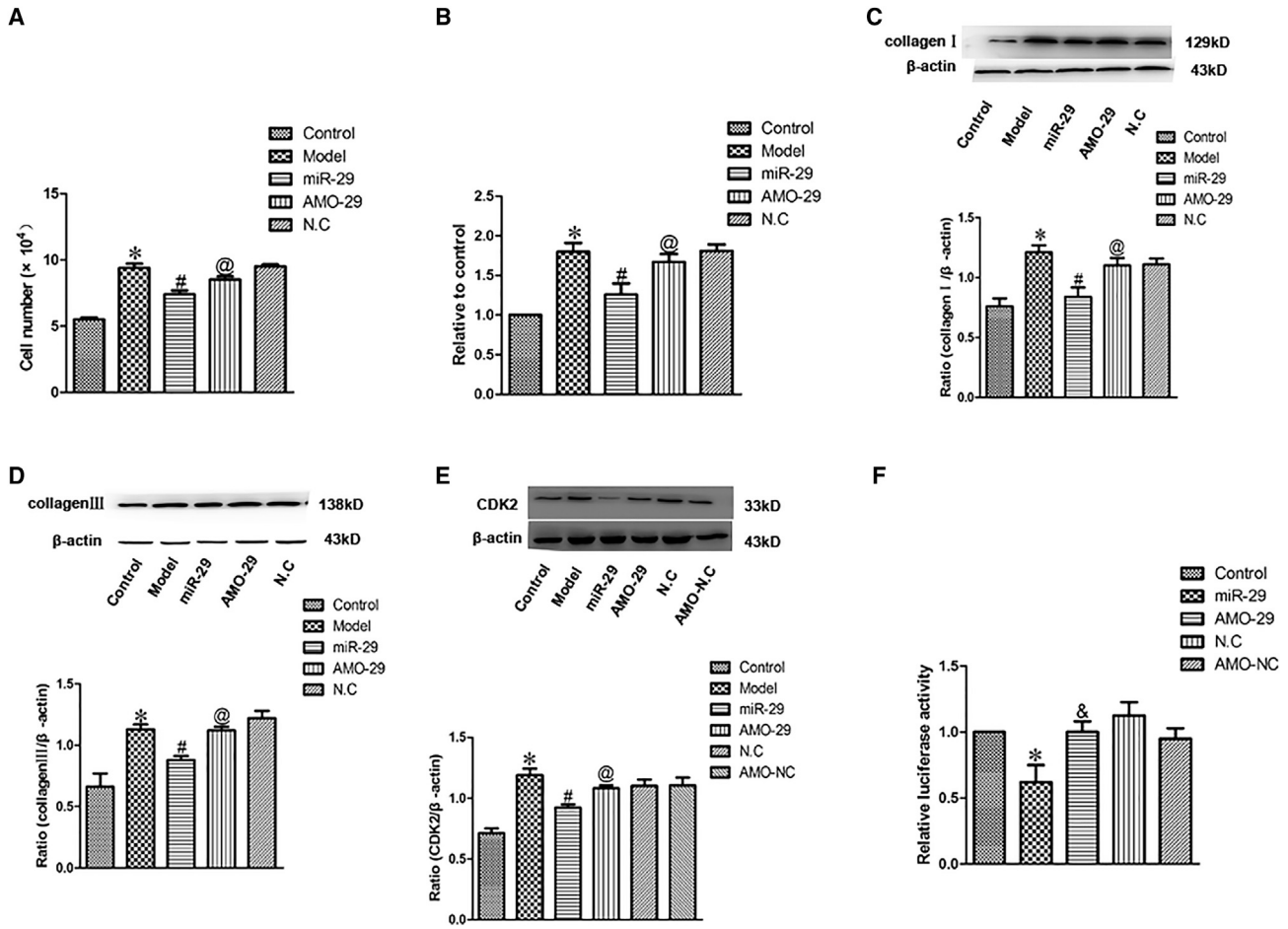

Figure 5. Anti-fibrotic Effects of miR-29 Family and Experimental Establishment of CDK2 as a Target of miR-29 Family

Overexpression of miR-29 family inhibited the proliferation of neonatal rat cardiac fibroblasts and the expressions of collagen I and collagen III proteins. (A) Cell number counting. (B) MTT test. (C) Western blot assay for collagen I expression in cardiac fibroblasts. (D) Western blot assay for collagen III expression in cardiac fibroblasts. (E) Effect of miR-29 family on the protein expression of CDK2 in cultured neonatal rat cardiac fibroblasts. (F) Luciferase reporter activities of chimerical vectors carrying luciferase gene and a fragment of CDK2 3′ UTR from rat containing the binding sites of miR-29 family. miR-29 group: cardiac fibroblasts were transfected with miR-29a, b, and c for 24 hr after treatment with Ang II for 24 hr; AMO-29 group: cells were co-transfected with miR-29a, b, and c and AMO-29a, b, and c for 24 hr after treatment with Ang II for 24 hr; NC group: cells were transfected with a random sequence for 24 hr after treatment with Ang II for 24 hr; and AMO-NC group: cells were transfected with a random sequence for 24 hr after treatment with Ang II for 24 hr. AMO-NC and NC indicated negative control. The results are mean ± SEM. *$p < 0.05$ versus control group; $^{\#}p < 0.05$ versus model group; and $^{@}$ or $^{\&}p < 0.05$ versus miR-29 group.

regulatory proteins. Intriguingly, the expressions of p21 and p27, the cyclin-dependent kinase inhibitors, were strongly induced by AMPK activation (AICAR or A769662), and this effect was abolished in the presence of the AMPK antagonist (compound C). Moreover, by silencing (knockdown) either p21 or p27, the DNA synthesis was at least partially restored, whereas by knockdown of both of p21 and p27, the DNA synthesis was almost restored back to the level seen at model control, indicating that p21 and p27 are indeed involved in mediating the inhibition of cardiac fibroblasts proliferation by AMPK activation in AICAR-treated cells.

miRNAs, as regulators of a wide range of biological processes, offer additional post-transcriptional checkpoints in gene regulation.[26] Overexpression of miRNAs is a common phenomenon that occurs in various diseases, and abnormally expressed miRNAs often participate in the pathogenesis of specific diseases, including heart disease. For example, miR-21, miR-23a, miR-24, miR-125, miR-129, miR-195, miR-199, miR-208, and miR-212 are often upregulated, whereas miR-1, miR-133, miR-29, miR-30, and miR-150 are often downregulated in cardiac hypertrophy. At same time, miR-1 and miR-133 increase arrhythmogenesis in heart failure. It can be seen that miRNAs are very important for the regulation of heart disease. Recently, a great deal of research has shown that miR-29b inhibits fibrosis by directly targeting mRNA 3′ UTR of many genes encoding fundamental membrane collagens, including Col 1a1, Col 5a3, and Col 4a2.[17,27–29] However, there is no direct evidence indicating the role of AMPK and the

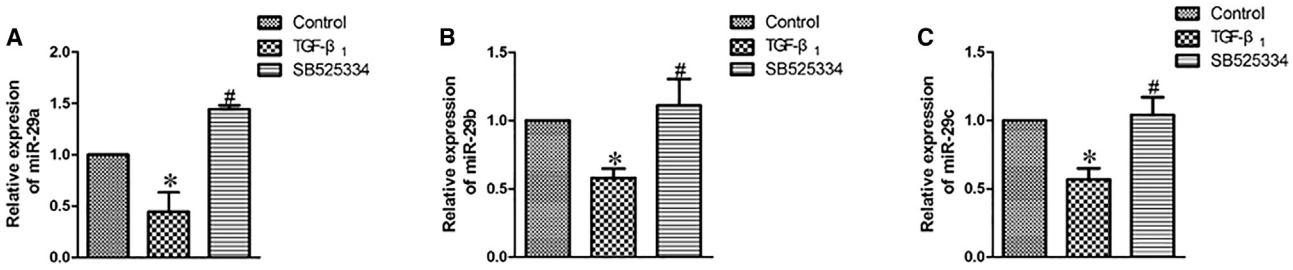

Figure 6. TGF-β_1 Inhibited miR-29 Family Expression in Cardiac Fibroblasts

(A–C) miR-29 expression was measured by quantitative real-time PCR using specific TaqMan probes and normalized to U6 after TGF-β_1 stimulation for 24 hr or co-treatment with SB525334. The results are mean ± SEM. *$p < 0.05$ versus control group and $^{\#}p < 0.05$ versus TGF-β_1 group.

miR-29 family or the underlying regulatory mechanisms between AMPK and the miR-29 family in the pathological process of cardiac fibrosis. In this study, AMPK activation by A769662 remarkably increased the expression of the miR-29 family compared with the model of cardiac fibroblasts, whereas, this effect could be reversed by compound C. Indeed, this result strongly revealed that there was an inevitable signal conditioning relationship between the AMPK and miR-29. In addition, we used both gain- and loss-of-function techniques on miR-29 family expression to explore the regulatory effect of the miR-29 family on anti-fibrotic action. We found that forcing overexpression of the miR-29 family could significantly repress the expression of collagen I and III proteins in vitro. On the contrary, the anti-miR-29 family significantly enhanced their expressions in cardiac fibroblasts. Furthermore, to explore direct miR-29 family targeting, miRanda software was used to predict the target genes of the miR-29 family. We also found that the cell cycle protein CDK2 was most likely a target gene for the miR-29 family simply because of the conservative sequence fragment among different species, which was fully supported by the notion that, by using a luciferase reporter gene assay, as well as protein expression detections, the CDK2 as a direct target of the miR-29 family was validated. Taking all of the data together reported here suggested that the miR-29 family protected against cardiac fibrosis via inhibition of cell cycle protein CDK2 expression, and then blocked the cell cycle of cardiac fibroblasts, and, finally, restrained the development of cardiac fibrosis. In our study, we confirmed the regulation effect of the miR-29 family on cardiac fibrosis, which was consistent with a previous study by van Rooij et al.[16] and validated another new target CDK2 beyond that. Most importantly, the miR-29 family expression could be enhanced by AMPK activation.

TGF-β_1 plays a key role in the development of tissue fibrosis.[29] TGF-β_1 stimulation induces conversion of fibroblasts to myofibroblasts[30] and enhances the production and deposition of collagens. Recent studies have shown that TGF-β_1 mediates fibrosis via miRNA-dependent mechanisms. Ramdas et al.[18] reported that TGF-β_1 repressed miR-29 expression in rat tubular epithelial NRK52E cells. In our study, enforcing overexpression of TGF-β_1 reduced the expression of the miR-29 family, and this effect could be reversed by SB525334 (TGF-β_1 receptor antagonist) in cardiac fibroblasts. Transcription factors represent the most numerous gene regulatory factors in the genomes of multi-cellular organisms. Furthermore, the JASPAR database analysis indicates that HNF-4α could bind to TGF-β_1 promoter regions. Together with the results from luciferase report assays and ChIP, our data demonstrated that HNF-4α regulated TGF-β_1 transcription. Simultaneously, HNF-4α expression was obviously inhibited by AMPK activation.

In summary, this study unraveled a novel role of AMPK in cardiac fibrosis. Activation of AMPK inhibited proliferation of cardiac fibroblasts and production of collagen in vivo and in vitro and improved the impaired cardiac function of hearts subjected to coronary artery ligation as well. Activation of AMPK, on the one hand, upregulated the expression of p21 and p27, further inhibited the CDK2 and cyclin E complex, and, finally, suppressed the progression of cardiac fibrosis. on the other hand, repressed HNF-4α expression, furthermore downregulated the activity of the TGF-β_1 promoter, and promoted downstream of miR-29 family expression, and, finally, prevented the development of cardiac fibrosis, as summarized in Figure 8E.

MATERIALS AND METHODS

Animals

Healthy male Wistar rats (weight, 200–250 g) used in the present study were kept under standard animal room conditions (temperature, 21 ± 1°C; humidity, 55%–60%) with food and water ad libitum for 1 week before the experiments. All animal protocols were approved by the Institutional Animal Care and Use Committee of the Harbin Medical University, PRC. All experimental procedures conformed to the Guide for the Care and Use of Laboratory Animals published by the US NIH (publication, 8th Edition, 2011). This study, including any relevant details, was approved by the Experimental Animal Ethic Committee of Harbin Medical University.

Myocardial Infarction Models

Rats were anesthetized with ketamine-xylazine (100 mg/kg, 5 mg/kg, intraperitoneally [i.p.]), then a stump needle was intubated orally for artificial respiration (UGO Basile S.R.L. Biological Research Apparatus). Left-sided thoracotomy was performed through the fourth

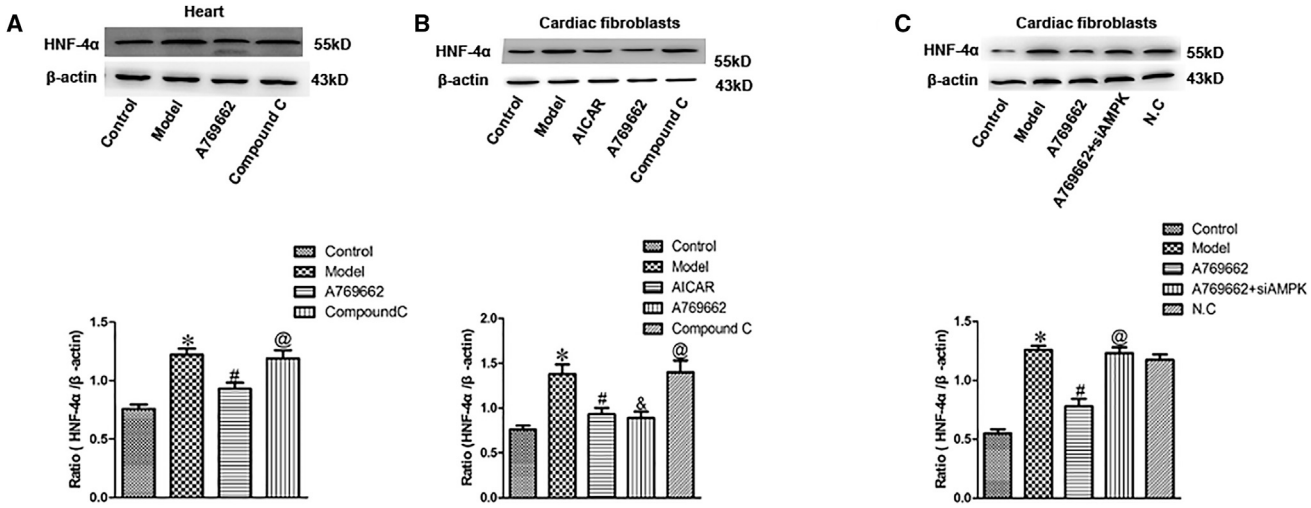

Figure 7. Activation of AMPK Promoted the Expression of HNF-4α in Cardiac Fibrosis Rat Hearts Induced by Left Coronary Artery Ligation and Cultured Cardiac Fibroblasts Administrated with Ang II 100 nmol/L

(A) Activation of AMPK suppressed the expression of HNF-4α in cardiac fibrosis rat hearts induced by left coronary artery ligation. (B) Activation of AMPK suppressed the expression of HNF-4α in cultured cardiac fibroblasts administrated with Ang II 100 nmol/L. (C) The inhibitory effect on HNF-4α expression was alleviated when silencing AMPK in cultured cardiac fibroblasts administrated with Ang II 100 nmol/L. siAMPK + A769662 group: cardiac fibroblasts were transfected with siAMPK for 24 hr before exposure to 300 μmol/L A769662 for 24 hr, following 24 hr treatment with Ang II and NC group: cells were transfected with a random sequence for 24 hr after treatment with Ang II for 24 hr. The results are mean ± SEM. *$p < 0.05$ versus control group; $^{\#}$ or $^{\&}p < 0.05$ versus model group; and $^{@}p < 0.05$ versus A769662 or AICAR group.

and fifth ribs, and the left descending coronary artery (LAD) was ligated using a 5/0 (for rats) prolene suture. Regional ischemia was confirmed by discoloration of the occluded distal myocardium and apparent S-T segment elevation in electrocardiogram (ECG). After surgery, the rats received food and water ad libitum. The cardiac infarction rats were randomly divided into three groups 2 weeks after cardiac infarction: (1) model group; (2) A769662 (molecular structure was shown in Figure S3A) group: cardiac infarction rats were injected intraperitoneally A769662 (agonist of AMPK, Sigma) at 0.84 g/kg/day for 1 week; and (3) compound C (molecular structure was shown in Figure S3B) group: 0.26 mg/kg/day compound C (antagonist of AMPK, Sigma) was administered intraperitoneally 2 hr before reinjection of A769662 for 1 week. The control group only received an injection of same amount of saline.

Hemodynamic Measurements

A pressure-volume control unit (Scisense) was used to measure hemodynamic indices. After the rats were anesthetized, a pressure-sensing catheter (1.9F, Scisense) was inserted into the left ventricle via the right common carotid artery. LVSP, LVEDP, maximum rate of left ventricular pressure rise and fall ($\pm dp/dt_{max}$) were examined. After functional measurement, rats were killed with overdose of sodium phenobarbital. The hearts were collected and dropped immediately into liquid nitrogen or 4% paraformaldehyde for the future use.

Histological Analysis of Collagen Deposition

The hearts were fixed in 4% paraformalin and cut into 5 μm thick sections. Masson's trichrome staining was used to evaluate collagen deposition. Sections were imaged at 200× magnification by bright-field microscopy (IX71, Olympus). The extent of cardiac fibrosis was assessed by calculating collagen volume fraction. Each observer examined a minimum of five (to eight) separate images from different (non-overlapping) regions. All quantitative evaluations were carried out by Image Pro Plus software (version 6.0, Media Cybernetics).

Neonatal Rat Cardiac Fibroblasts Isolation and Incubation

Neonatal rat cardiac fibroblasts were prepared from 2- to 3-day-old neonatal Wistar rats. The neonatal rats were anesthetized with dry ice (CO_2), and then immersed in 75% (v/v) ethanol. The ventricles were finely minced and placed together in 0.25% trypsin. Collected cell suspensions were centrifuged and resuspended in DMEM (Gibco and Thermo Fisher Scientific) supplemented with 10% fetal bovine serum (FBS, Gibco and Thermo Fisher Scientific). The resuspension was plated onto culture flasks for 90 min, which allowed for preferential attachment of fibroblasts to the bottom of the culture flasks. Then, cardiac fibroblasts were cultured at 37°C in a humidified atmosphere containing 5% (v/v) CO_2. Cardiac fibroblasts at the third or fourth passage were used in the experiments. Neonatal rat cardiac fibroblasts were randomly divided into ten groups: (1) control group; (2) model group: cells were incubated with Ang II (100 nmol/L) for 24 hr; (3) AICAR (molecular structure was shown in Figure S3C) group: cells were given 500 μmol/L AICAR for 24 hr after treatment with Ang II (100 nmol/L) for 24 hr; (4) A769662 group: cells were given 300 μmol/L A769662 for 24 hr after treatment with Ang II (100 nmol/L) for 24 hr; (5) compound C group: 80 μmol/L compound C was administered for 2 hr before exposure to 300 μmol/L A769662

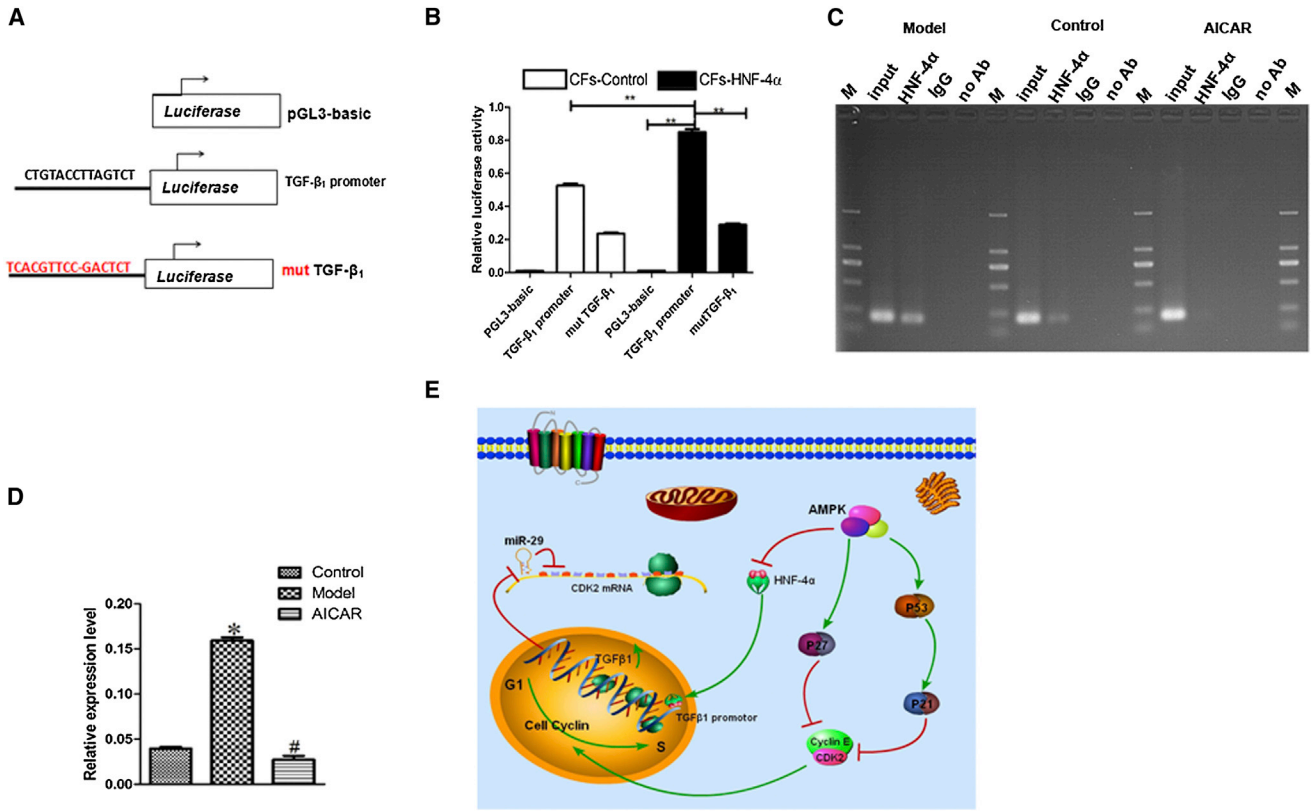

Figure 8. TGF-β_1 Was the Direct Target of HNF-4α in Cardiac Fibroblasts

Verification of TGF-β_1 as a HNF-4α target via luciferase reporter assays. (A) Constructs with an intact TGF-β_1 promoter resulted in enhanced luciferase activities in HNF-4α-expressing cardiac fibroblasts (CFs), while those carrying a mutant site resulted in strongly repressed luciferase activities. (B) In contrast with CFs-HNF-4α cells, CFs-Control failed to show any luciferase activity after transfection with any of the above constructs. ChIP-PCR confirmed that HNF-4α bound to the TGF-β_1 promoter in vivo. (C) Amplification of the TGF-β_1 promoter sequence from the ChIP DNA validated the binding of HNF-4α to the TGF-β_1 promoter. Sonicated input DNA and no Ab lanes served as positive and negative controls, respectively. (D) TGF-β_1 promoter activity diagram. The product sequences were terminally verified to represent the TGF-β_1 promoter following gene-sequencing analysis. (E) Schematic diagram for the proposed AMPK-anti-fibrotic signaling pathways. The average data were represented by mean ± SEM. $^{*}p < 0.05$ versus control group and $^{\#}p < 0.05$ versus model group.

for 24 hr, following 24 hr treatment with Ang II (100 nmol/L); (6) siAMPK + A769662 group: neonatal rat cardiac fibroblasts were transfected with siAMPK (10 μmol/L) for 24 hr before exposure to 300 μmol/L A769662 for 24 hr, following 24 hr treatment with Ang II (100 nmol/L); (7) miR-29 group: neonatal rat cardiac fibroblasts were transfected with miR-29a, b, and c for 24 hr after treatment with Ang II (100 nmol/L) for 24 hr; (8) AMO-29 group: cells were co-transfected with miR-29a, b, and c and AMO-29a, b, and c for 24 hr after treatment with Ang II (100 nmol/L) for 24 hr; (9) negative control (NC) group: cells were transfected with a random sequence for 24 hr after treatment with Ang II (100 nmol/L) for 24 hr; and (10) AMO-NC group: cells were transfected with a random sequence for 24 hr after treatment with Ang II (100 nmol/L) for 24 hr.

Western Blot

Protein samples (50 μg) were separated in SDS-PAGE and transferred onto nitrocellulose membrane. The blots were blocked with 5% non-fat milk for 2 hr at room temperature, then incubated with primary antibody including p21 (1:200 dilution, Abcam, ab109520), p27 (1:200 dilution, Abcam, ab60019), CDK2 (1:200 dilution, ab101682, Abcam), cyclin E (1:200 dilution, Abcam, ab1108), HNF-4α (1:200 dilution, Abcam, ab136861), type I collagen (collagen I, 1:200 dilution, Abcam, ab34710), type III collagen (collagen III, 1:200 dilution, Abcam, ab82354), TGF-β_1 (1:200 dilution, Abcam, ab92486), and β-actin (1:5,000 dilution, Kangcheng, KC5A08), respectively, at 4°C overnight. The western blot bands were collected by Imaging System (LI-COR Biosciences) and quantified with Odyssey v.1.2 software by measuring intensity (area × optical density [OD]) in each group with β-actin as internal control.

Quantitative Real-Time PCR

Total RNA from cultured fibroblasts were extracted using TRIzol reagent (Invitrogen) following the manufacturer's protocol. cDNA was synthesized by a High-Capacity cDNA Reverse Transcription Kit (Applied Biosystems). The levels of miR-29 were determined using the SYBR Green I incorporation method on an ABI 7500

Fast Real-Time PCR System (Applied Biosystems), with Rnu6 (U6) as an internal control. Relative quantification of gene expression was performed with the $2^{-\Delta\Delta Ct}$ method. The sequences of primers were as follows:

miR-29a: Forward: GCGGCGGTAGCACCATCTGAAATC

reverse: ATCCAGTGCAGGGTCCGAGG

reverse transcriptase primer: GTCGTATCCAGTGCAGGGTCC GAGGTATTCGCACTGGATACGACCTGAAC

miR-29b: Forward: GCGGCGGCTGGTTTCACATGGTG

reverse: ATCCAGTGCAGGGTCCGAGG

reverse transcriptase primer: GTCGTATCCAGTGCAGGGTCC GAGGTATTCGCACTGGATACGACCTAAGC

miR-29c: Forward: GCGGCGGTGACCGATTTCTCCTG

reverse: ATCCAGTGCAGGGTCCGAGG

reverse transcriptase primer: GTCGTATCCAGTGCAGGGTCC GAGGTATTCGCACTGGATACGACGAACAC.

Cell Cycle Analysis

Cell cycle progression was assessed by flow cytometry as reported previously.[31] Cardiac fibroblasts were collected and suspended in PBS. Fibroblast pellets were centrifuged at 1,000 *g* for 5 min and washed twice with PBS, resuspended in 70% ethanol, and fixed at 4°C for overnight. Fixed cells were then incubated with propidium iodide (50 μg/mL) and RNase A (100 μg/mL) for 30 min at room temperature, and DNA fluorescence was measured by ELITE Flow Cytometry (BD Biosciences) and CellQuest software (BD Biosciences).

Cell Proliferation and DNA Synthesis

Cardiac fibroblasts from neonatal rat were seeded (2×10^6 cells/well) onto 6-well plates in serum-containing media. After 24 hr, cells were washed and treated with serum-containing media in the presence and absence of various test compounds.

Cell number determinations were performed at various times by dissociating cells with trypsin and counting cells in a Beckman Z1 Coulter Counter (Beckman Coulter). For detection of cardiac fibroblast proliferation by measuring DNA synthesis, cells were incubated with [^{3}H]thymidine for 4 hr, washed three times with ice-cold PBS, and fixed with 10% trichloracetic acid at 4°C for 30 min. DNA was then extracted with 0.2% SDS/0.2 N NaOH and radioactivity was determined by scintillation spectroscopy.

MTT Assay

The cardiac fibroblasts were seeded in a 96-well plate at a density of 5×10^3 cells per well. Then, the cells were added to various concentrations of AICAR. After 24 hr, each well was added in 20 μL of MTT (5 mg/mL) and incubated at 37°C for 4 hr. Finally, the culture supernatant was removed, each well was supplemented with 150 μL of DMSO and shaken in darkness for 10 min. Samples were then measured at 570 nm.

siRNA Treatment

siRNA duplex sequences corresponding to p21 (GCCTTAGTC TCAGTTTGTGTGTCTT), p27 (GTACGAGTGGCAAGAGGUG), and a non-specific control (TTCGTAAGAGACCGTGGATCCT GTC) were prepared, respectively, as described by the manufacturer (Sequitur). Cardiac fibroblasts were grown in medium lacking doxycycline for 24 hr, and then transfected with siRNAs (25 μmol/L) using Oligofectamine according to the manufacturer's instructions (Invitrogen). The siRNA sequences used for targeted silencing of rat α1/α2 AMPK isoforms (sc-45312) were supplied by Santa Cruz Biotechnology.

Synthesis of miR-29a/b/c and Anti-miR-29a/b/c Antisense Inhibitors

miR-29a, miR-29b, miR-29c, and their antisense oligonucleotides, AMO-29a, AMO-29b, and AMO-29c were synthesized by GenePharma (Shanghai GenePharma). The sequences were as follows:

miR-29a: sense: 5′-UAGCACCAUCUGAAAUCGGUUA-3′

antisense: 5′-ACCGAUUUCAGAUGGUGCUAUU-3′

miR-29b: sense: 5′-UAGCACCAUUUGAAAUCAGUGUU-3′

antisense: 5′-CACUGAUUUCAAAUGGUGCUAUU

miR-29c: sense: 5′-UAGCACCAUUUGAAAUCGGUUA-3′

antisense: 5′-ACCGAUUUCAAAUGGUGCUAUU-3′

NC: sense: 5′-UUCUCCGAACGUGUCACGUTT-3′

antisense: 5′-ACGUGACACGUUCGGAGAATT-3′

AMO-miR-29a: 5′-UAACCGAUUUCAGAUGGUGCUA-3′

AMO-miR-29b: 5′- AACACUGAUUUCAAAUGGUGCUA-3′

AMO-miR-29c: 5′-UAACCGAUUUCAAAUGGUGCUA-3′

AMO-NC: 5′-CAGUACUUUUGUGUAGUACAA-3′.

All pyrimidine nucleotides in the NC or miR-29a, b, and c were substituted by their 2′-O-methyl analogs to improve RNA stability. Transfection of synthesized RNAs was accomplished using X-tremeGENE siRNA Transfection Reagent (Roche) according to the manufacturer's protocol.

Construction of Rat CDK2 Overexpression Vector

The protein encoding sequence of the CDK2 mRNA (NM_199501) was amplified. The obtained CDK2 mRNA sequence was then cloned into a pEGFP-N1 vector (pEGFP-N1-CDK2-GFP) containing a cytomegalovirus promoter. The empty pEGFP-N1 plasmid was used as a negative control.

Luciferase Assays

To construct reporter vectors bearing miRNA-target sites, we first obtained fragments of the 3′ UTRs of CDK2 containing the exact target sites for the miR-29 family by PCR amplification. CDK2 3′ UTRs were inserted into the multiple cloning sites at downstream of the

luciferase gene (HindIII and SacI sites) in the pMIR-REPORTTM luciferase miRNA expression reporter vector (Ambion) to form a chimeric plasmid. After that, 1 μg chimeric plasmid (firefly luciferase vector), 0.1 μg PRL-TK (TK-driven Renilla luciferase expression vector), and the appropriate miRNAs or their inhibitors were co-transfected with lipofectamine 2000 (Invitrogen) into HEK293 cells (1×10^5/well). Luciferase activities were measured with a Dual-Luciferase Reporter Assay Kit (Promega) on a Luminometer (GloMax 20/20) at 48 hr following transfection. For all experiments, transfection took place 24 hr after the starvation of cells in serum-free medium. The normalized luciferase activity relative to the control group was used to demonstrate the alteration of mRNA transcription.

ChIP

ChIP assays were carried out using an anti-HNF-4α antibody (Santa Cruz Biotechnology). Ten percent of chromatin prior to immunoprecipitation was used as input controls and non-specific antibody (rabbit anti-immunoglobulin G [IgG]; BD Biosciences) served as negative controls. The precipitated DNAs were subjected to PCR in attempt to amplify the HNF-4α-binding sites using primers specific for TGF-β_1 promoter (forward: 5′CAACGTAAAAGGGCTGTACCT3′ and reverse: 5′AGCCATAGCCAGCAAGCTGG 3′). The amplified fragments were then resolved electrophoretically on a 2% (w/v) agarose gel and verified by DNA sequencing.

Data Analysis

All data were analyzed statistically by one-way ANOVA followed by the Tukey multiple-comparisons test (SPSS 15.0). Average data were represented by mean ± SEM. Differences were considered as statistically significant when $p < 0.05$.

SUPPLEMENTAL INFORMATION

Supplemental Information includes three figures and can be found with this article online at http://dx.doi.org/10.1016/j.omtn.2017.07.004.

AUTHOR CONTRIBUTIONS

Conceived and designed the experiments: H.S. Performed the experiments: H.Q., Y.L., S.L., Y.C., L.L., Y.C., M.E., P.S., C.S., and B.L. Analyzed the data: H.Q. and H.S. Wrote the paper: H.Q., B.L., and H.S.

CONFLICTS OF INTEREST

None declared.

ACKNOWLEDGMENTS

This study was supported by the Yu Weihan Outstanding Youth Training Fund of Harbin Medical University (to H.S.), the Natural Science Foundation of Heilongjiang Province (H2015108 to H.Q.), the Wu Liande Fund of Harbin Medical University (Daqing) (DQWLD201603 to H.Q.), the Seed Fund of Harbin Medical University (Daqing) (DQ2014-02 to H.Q.), and the Project of Science and Technology Bureau of Daqing (zdy-2016-081 to H.Q.).

REFERENCES

1. Krenning, G., Zeisberg, E.M., and Kalluri, R. (2010). The origin of fibroblasts and mechanism of cardiac fibrosis. J. Cell. Physiol. *225*, 631–637.
2. Carver, W., Terracio, L., and Borg, T.K. (1993). Expression and accumulation of interstitial collagen in the neonatal rat heart. Anat. Rec. *236*, 511–520.
3. Hardie, D.G., Hawley, S.A., and Scott, J.W. (2006). AMP-activated protein kinase–development of the energy sensor concept. J. Physiol. *574*, 7–15.
4. Kudo, N., Barr, A.J., Barr, R.L., Desai, S., and Lopaschuk, G.D. (1995). High rates of fatty acid oxidation during reperfusion of ischemic hearts are associated with a decrease in malonyl-CoA levels due to an increase in 5′-AMP-activated protein kinase inhibition of acetyl-CoA carboxylase. J. Biol. Chem. *270*, 17513–17520.
5. Kudo, N., Gillespie, J.G., Kung, L., Witters, L.A., Schulz, R., Clanachan, A.S., and Lopaschuk, G.D. (1996). Characterization of 5'AMP-activated protein kinase activity in the heart and its role in inhibiting acetyl-CoA carboxylase during reperfusion following ischemia. Biochim. Biophys. Acta *1301*, 67–75.
6. Zhou, G., Myers, R., Li, Y., Chen, Y., Shen, X., Fenyk-Melody, J., Wu, M., Ventre, J., Doebber, T., Fujii, N., et al. (2001). Role of AMP-activated protein kinase in mechanism of metformin action. J. Clin. Invest. *108*, 1167–1174.
7. Russell, R.R., 3rd, Li, J., Coven, D.L., Pypaert, M., Zechner, C., Palmeri, M., Giordano, F.J., Mu, J., Birnbaum, M.J., and Young, L.H. (2004). AMP-activated protein kinase mediates ischemic glucose uptake and prevents postischemic cardiac dysfunction, apoptosis, and injury. J. Clin. Invest. *114*, 495–503.
8. Shibata, R., Sato, K., Pimentel, D.R., Takemura, Y., Kihara, S., Ohashi, K., Funahashi, T., Ouchi, N., and Walsh, K. (2005). Adiponectin protects against myocardial ischemia-reperfusion injury through AMPK- and COX-2-dependent mechanisms. Nat. Med. *11*, 1096–1103.
9. Matsui, Y., Takagi, H., Qu, X., Abdellatif, M., Sakoda, H., Asano, T., Levine, B., and Sadoshima, J. (2007). Distinct roles of autophagy in the heart during ischemia and reperfusion: roles of AMP-activated protein kinase and Beclin 1 in mediating autophagy. Circ. Res. *100*, 914–922.
10. Terai, K., Hiramoto, Y., Masaki, M., Sugiyama, S., Kuroda, T., Hori, M., Kawase, I., and Hirota, H. (2005). AMP-activated protein kinase protects cardiomyocytes against hypoxic injury through attenuation of endoplasmic reticulum stress. Mol. Cell. Biol. *25*, 9554–9575.
11. Lopaschuk, G.D. (2008). AMP-activated protein kinase control of energy metabolism in the ischemic heart. Int. J. Obes. *32* (*Suppl 4*), S29–S35.
12. Chan, A.Y., Soltys, C.L., Young, M.E., Proud, C.G., and Dyck, J.R. (2004). Activation of AMP-activated protein kinase inhibits protein synthesis associated with hypertrophy in the cardiac myocyte. J. Biol. Chem. *279*, 32771–32779.
13. Yang, B., Lin, H., Xiao, J., Lu, Y., Luo, X., Li, B., Zhang, Y., Xu, C., Bai, Y., Wang, H., et al. (2007). The muscle-specific microRNA miR-1 regulates cardiac arrhythmogenic potential by targeting GJA1 and KCNJ2. Nat. Med. *13*, 486–491.
14. Carè, A., Catalucci, D., Felicetti, F., Bonci, D., Addario, A., Gallo, P., Bang, M.L., Segnalini, P., Gu, Y., Dalton, N.D., et al. (2007). MicroRNA-133 controls cardiac hypertrophy. Nat. Med. *13*, 613–618.
15. Sayed, D., Hong, C., Chen, I.Y., Lypowy, J., and Abdellatif, M. (2007). MicroRNAs play an essential role in the development of cardiac hypertrophy. Circ. Res. *100*, 416–424.
16. van Rooij, E., Sutherland, L.B., Qi, X., Richardson, J.A., Hill, J., and Olson, E.N. (2007). Control of stress-dependent cardiac growth and gene expression by a microRNA. Science *316*, 575–579.
17. van Rooij, E., Sutherland, L.B., Liu, N., Williams, A.H., McAnally, J., Gerard, R.D., Richardson, J.A., and Olson, E.N. (2006). A signature pattern of stress-responsive microRNAs that can evoke cardiac hypertrophy and heart failure. Proc. Natl. Acad. Sci. USA *103*, 18255–18260.
18. Ramdas, V., McBride, M., Denby, L., and Baker, A.H. (2013). Canonical transforming growth factor-β signaling regulates disintegrin metalloprotease expression in experimental renal fibrosis via miR-29. Am. J. Pathol. *183*, 1885–1896.
19. Tsuda, T., Gao, E., Evangelisti, L., Markova, D., Ma, X., and Chu, M.L. (2003). Post-ischemic myocardial fibrosis occurs independent of hemodynamic changes. Cardiovasc. Res. *59*, 926–933.
20. Qi, H.P., Wang, Y., Zhang, Q.H., Guo, J., Li, L., Cao, Y.G., Li, S.Z., Li, X.L., Shi, M.M., Xu, W., et al. (2015). Activation of peroxisome proliferator-activated receptor γ

(PPARγ) through NF-κB/Brg1 and TGF-β1 pathways attenuates cardiac remodeling in pressure-overloaded rat hearts. Cell. Physiol. Biochem. *35*, 899–912.

21. Fan, Z., and Guan, J. (2016). Antifibrotic therapies to control cardiac fibrosis. Biomater Res *20*, 13.
22. Kang, L.L., Zhang, D.M., Ma, C.H., Zhang, J.H., Jia, K.K., Liu, J.H., Wang, R., and Kong, L.D. (2016). Cinnamaldehyde and allopurinol reduce fructose-induced cardiac inflammation and fibrosis by attenuating CD36-mediated TLR4/6-IRAK4/1 signaling to suppress NLRP3 inflammasome activation. Sci. Rep. *6*, 27460.
23. Wang, J.D., and Levin, P.A. (2009). Metabolism, cell growth and the bacterial cell cycle. Nat. Rev. Microbiol. *7*, 822–827.
24. Elledge, S.J. (1996). Cell cycle checkpoints: preventing an identity crisis. Science *274*, 1664–1672.
25. Nigg, E.A. (1995). Cyclin-dependent protein kinases: key regulators of the eukaryotic cell cycle. BioEssays *17*, 471–480.
26. Bartel, D.P. (2004). MicroRNAs: genomics, biogenesis, mechanism, and function. Cell *116*, 281–297.
27. Li, Z., Hassan, M.Q., Jafferji, M., Aqeilan, R.I., Garzon, R., Croce, C.M., van Wijnen, A.J., Stein, J.L., Stein, G.S., and Lian, J.B. (2009). Biological functions of miR-29b contribute to positive regulation of osteoblast differentiation. J. Biol. Chem. *284*, 15676–15684.
28. Luna, C., Li, G., Qiu, J., Epstein, D.L., and Gonzalez, P. (2009). Role of miR-29b on the regulation of the extracellular matrix in human trabecular meshwork cells under chronic oxidative stress. Mol. Vis. *15*, 2488–2497.
29. Lijnen, P.J., Petrov, V.V., and Fagard, R.H. (2000). Induction of cardiac fibrosis by transforming growth factor-beta(1). Mol. Genet. Metab. *71*, 418–435.
30. Evans, R.A., Tian, Y.C., Steadman, R., and Phillips, A.O. (2003). TGF-beta1-mediated fibroblast-myofibroblast terminal differentiation-the role of Smad proteins. Exp. Cell Res. *282*, 90–100.
31. Keswani, A.N., Peyton, K.J., Durante, W., Schafer, A.I., and Tulis, D.A. (2009). The cyclic GMP modulators YC-1 and zaprinast reduce vessel remodeling through antiproliferative and proapoptotic effects. J. Cardiovasc. Pharmacol. Ther. *14*, 116–124.